lubricants

MDPI

Article

Low-Foaming/Aeration and Low-Traction Electric Drivetrain Fluid (EDF) Solutions for High-Speed E-Mobility

Philip Ma *, Donna Mosher and Chad Steele

BASF Corporation, 500 White Plains Road, Tarrytown, New York, NY 10591, USA; donna.mosher@basf.com (D.M.); chad.steele@basf.com (C.S.)
* Correspondence: philip.ma@basf.com

Abstract: The use of electrically driven drivetrains is increasing for passenger cars and light-, medium-, and heavy-duty trucks. Off-the-shelf automatic transmission fluids (ATFs) are still being used as electric drivetrain fluids (EDFs). EDFs are trending toward lower viscosity for better energy efficiency and better heat transfer capacity, while satisfying all the other challenging requirements, such as gear/bearing scuffing/wear protection, oxidative stability, copper corrosion, and coating/seal material compatibility. In this paper, we will highlight the importance of low foaming, low aeration, and low traction coefficient which are critical for the performance of the EDF during high-speed applications, measured using metrics such as energy efficiency, heat transfer capacity, and longer oil drain interval.

Keywords: foaming; aeration; traction coefficient; fast FZG; energy efficiency; heat transfer capacity; long oil drain interval

1. Introduction

As electric vehicles (EVs) continue to gain traction in the automotive industry, EVs with higher motor rpm, higher torque, higher battery power, and longer drive range all pose continuous challenges for electric drivetrains and EDFs. Many OEMs are using off-the-shelf ATFs as lubricants for electric drivetrains, and they were shown to be safe to use [1]. Newly developed EDFs in the market are mostly focused on optimizing sulfur and phosphorus chemistry to balance the copper corrosion and load carry capacity for gear and bearing wear and scuffing protection.

The latest SAE J3200 (issued in October 2022) defines "Fluid for Automotive Electrified Drivetrains", particularly emphasizing the EDF's high-speed aeration properties and providing direction and guidance toward new EDF development. In comparison to conventional drivetrains, the electric drivetrain has a much higher rpm, smaller oil sump size and higher temperature. E-motor speed can exceed 20,000 rpm, leading to high air content/aeration as foam/entrained air. Under the high rpm and high turbulence, foaming/aeration can pose a significant challenge. Foaming/aeration occurs due to various factors, including high fluid turbulence, presence of surfactant or contaminants, aging, and type of lubricants. In electric drivetrains, where precise lubrication is critical for minimizing friction and heat management, dedicated EDFs should be designed for the high e-motor speed, with better heat transfer, material compatibility including coatings, seals, energy efficiency, better oxidative stability; thus, long oil drain intervals are still desired [2].

EDF is trending toward lower viscosity. The main driver for this trend is for better heat transfer capacity for direct cooling of the e-motor. Cooling the e-motor is paramount as higher battery power, higher e-motor torque, and higher vehicle acceleration/deceleration

check for updates

Received: 11 December 2024
Revised: 3 January 2025
Accepted: 16 January 2025
Published: 28 January 2025

Citation: Ma, P.; Mosher, D.; Steele, C. Low-Foaming/Aeration and Low-Traction Electric Drivetrain Fluid (EDF) Solutions for High-Speed E-Mobility. *Lubricants* **2025**, *13*, 53. https://doi.org/10.3390/lubricants13020053

speed all lead to higher e-motor temperature, and negatively impact vehicle range, electric drivetrain electronics and component life. Poor heat transfer will also affect EDF oxidative stability and further worsen heat transfer capacity, coating compatibility, scuffing/wear protection, efficiency. Although most systems have a cooling mechanism typically from the battery coolant looped to cool the e-motor, the heat transfer capacity of the EDF is still important.

Mouromtseff number (Mo) is a useful figure of merit (FOM) to compare the heat transfer capacity of various types of fluids [3,4]. For fluid flow over or through a given geometry at a specified velocity, the larger the Mo, the better the fluid's heat transfer capacity. For the single-phase forced convection, Mo can be expressed as

$$\mathrm{Mo} = \frac{\rho^{a} \cdot \mathrm{K}^{b} \cdot \mathrm{C_p}^{d}}{\mu^{e}}$$

where ρ is the fluid density, K is the fluid thermal conductivity, C_p is fluid-specific heat capacity, and μ is fluid dynamic viscosity, at given temperature and pressure.

Under high-speed rpm conditions of the electric drivetrain, the heat transfer capacity of EDF is of a turbulent mode to cool the motor. There are many models using different coefficients of *a*, *b*, *c*, *d* to calculate Mo [5–7]. People also frequently use different units for ρ, K, C_p, and μ, all affecting the Mo figure. However, the figure of merit does not affect the ranking of relative heat transfer capacity; under the same model, the higher the Mo, the better the heat transfer capacity. For example, water has excellent heat transfer capacity in comparison to common organic heat transfer fluids (HTFs), and its properties are well studied [8]; it is easier to normalize Mo for the testing fluid against water for better comparison which will not be affected by different units for ρ, K, C_p, and μ.

The differences in thermal conductivity K and specific heat C_p among different types of base stocks commonly used as lubricants, such as Group II/II+, Group III, Group IV (PAO), and Group V (esters, polyalkyleneglycols, etc.), do not make a huge impact toward Mo; the largest contributing factor affecting Mo is fluid viscosity. Typically, the lower the viscosity, the higher the Mo, as shown when calculated from the original Mouromtseff equation (Table 1).

$$\mathrm{Mo} = \frac{\rho^{0.80} \cdot \mathrm{K}^{0.67} \cdot \mathrm{C_p}^{0.33}}{\mu^{0.47}}$$

Table 1. Mo number calculated for saturated fluid (no aeration) internal turbulent flow model [ρ: kg/m^3, K: W/(m·K), C_p: kJ/(kg·K), μ: cP] at 100 °C at 1 atm.

Properties @ 100 °C		**Heat Transfer Fluid A**	**Heat Transfer Fluid B**	**EDF-3**	**EDF-4**
Description	**Water**	Aromatics	C14-30 alkylate	PAO-based	PAO-based
ρ, Density, kg/m^3	958	981	817	823	826
K, Thermal conductivity, W/(m·K)	0.680	0.117	0.116	0.134	0.134
C_p, Specific heat capacity, kJ/(kg·K)	4.217	1.843	2.203	2.229	2.229
μ, Dynamic viscosity, cP	0.279	1.690	2.610	3.640	4.914
Kinematic viscosity, cSt	0.29	1.72	3.19	4.42	5.95
Mo number	519.2	56.0	41.7	40.1	34.9
Mo number normalized against water	1.000	0.102	0.076	0.073	0.064

Air is a poor heat transfer media. In comparison to lubricant fluids, its heat transfer capacity is negligible. High air content in the fluid functions as a barrier to dissipate the heat from the system. Even though there is no model to calculate the Mo number of fluids with

high aeration, one can see that the aeration reduces the fluid density, thermal conductivity, and specific heat at the same time, thus greatly reducing the Mo number. We can use the same concept to estimate the aeration impact to Mo as a figure of merit (Table 2). High aeration will greatly reduce the Mo number and thus the fluid's heat transfer capacity.

Table 2. Mo number calculated for commercial heat transfer fluid A [9] with various amounts of air content under internal turbulent flow model [ρ: kg/m^3, K: W/(m·K), C_p: kJ/(kg·K), μ: cP] at 100 °C at 1 atm.

Properties @ 100 °C	**Heat Transfer Fluid A**	**Heat Transfer Fluid A**	**Heat Transfer Fluid A**	**Heat Transfer Fluid A**
Description	0% aeration	10% aeration	20% aeration	30% aeration
ρ, Density, kg/m^3	981	883	785	687
K, Thermal conductivity, W/(m·K)	0.117	0.105	0.093	0.082
C_p, Specific heat capacity, kJ/(kg·K)	1.843	1.659	1.474	1.290
μ, Dynamic viscosity, cP	1.690	1.521	1.352	1.183
Kinematic viscosity, cSt	1.72	1.72	1.72	1.72
Mo number	56.0	48.7	41.7	34.9
Mo number normalized against water	0.102	0.089	0.076	0.064

Figure 1 shows that aeration reduces Mo and reduces the EDF's heat transfer capacity. For example, for an EDF with kinematic viscosity at 100 °C, Kv100 is 3.0 cSt. A typical 20% aeration under the high-speed rpm dynamic condition will significantly drop its heat transfer capacity (Mo number) to a value equal to that of an EDF with Kv100 = 6.0 cSt with no aeration.

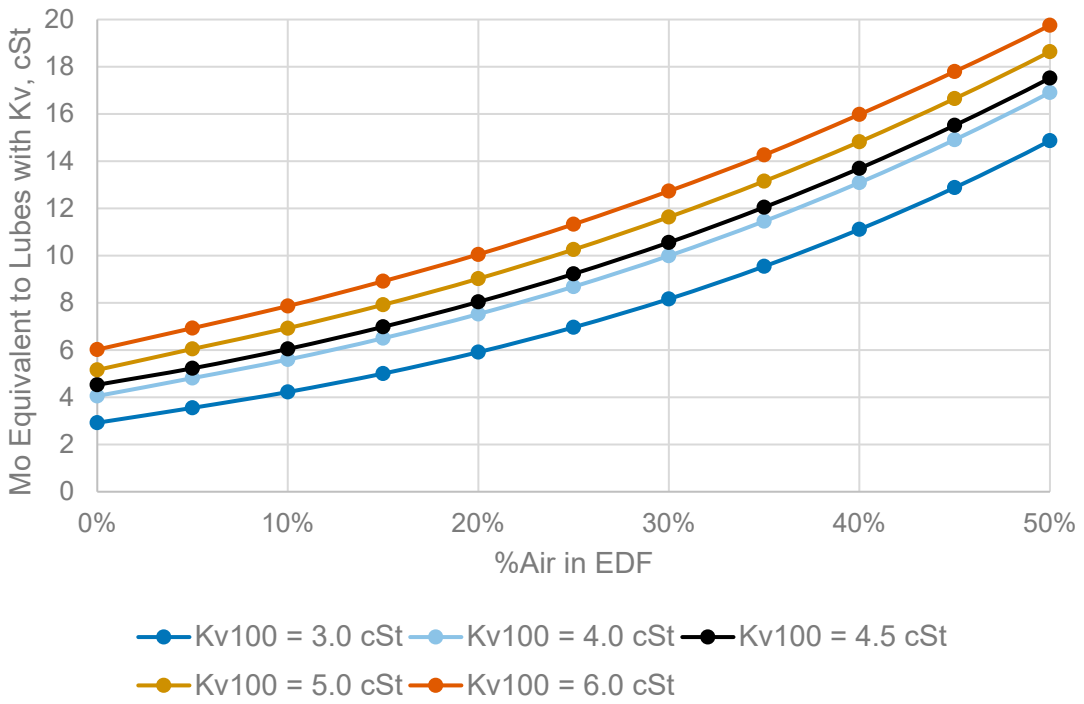

Figure 1. Mo number normalized against water calculated for internal turbulent flow mode using lab-generated data for low-viscosity PAO-based EDF candidates. Showing the impact of the % aeration under the high-speed dynamic condition on the heat transfer capacity of the EDF correlates to the heat transfer capacity of the EDF under the static state with no aeration.

The prevalent e-motor bearing premature failure is due to electric induced bearing damage (EIBD) [10–15]. Electric motors fitted with Variable Frequency Drives (VFDs) are at risk of bearing damage due to a build-up of current in the rotor that discharges through the shaft through the bearing–raceway gap, electrically erodes the bearing surface and raceway in a fluted pattern and produces harmful vibration that eventually results in bearing failure. Air has low dielectric breakdown voltage [16]. Air bubbles in the EDF film between the bearing and bearing raceway are the weakest point for the electric current to break through. If lubricant film between the bearing and raceway can reduce the electric current to break through and reduce the EIBD, it would be a continuous film with low aeration and low water (water also has a low dielectric breakdown voltage). Lubricants with high aeration can also lead to higher churning losses [17].

More air–lubricant contact under higher temperature also encourages the lubricant oxidation and reduces lubricant oil drain interval. High air content of the EDF under the high-rpm driving condition severely reduces the EDF's heat transfer capacity, further worsening the lubricant oxidation degradation.

Research has shown that the lubricant friction coefficient is related to energy efficiency at higher speed where the lubricant is not under the boundary lubrication regime [18,19]. Traction is the ratio of the shear stress to the contact pressure in the lubricant contact zone. Lubricant traction is measured by a Mini Traction Machine (MTM) under various slide-to-roll ratios (SRR%), speeds, loads, and temperatures.

It is paramount to develop low-foaming/aeration/traction EDFs for the high-speed rpm application.

2. Experimental Methods

Foam is defined as a collection of bubbles formed in the liquid or on (at) its surface where the air (or gas) is the major component on a volumetric basis; this is visually measured under various temperatures in ASTM D892 [20].

Entrained air (or gas) is defined as a two-phase mixture of air (or gas) dispersed in a liquid in which the volume of the liquid is the major component, and this is measured by density under various temperatures in ASTM D3427 [21].

Under the high-speed rpm dynamic conditions, foaming/aeration is measured by Fast FZG, simulating the high-speed rpm running conditions, which measures the lubricant air content by volume increase under various rpm. Fast FZG tests were performed at APL Automobil-Prüftechnik Landau GmbH in Germany, using standard FZG gears type A10, max rpm 17,000.

The MTM was from PCS Instruments. Traction curves were collected from 0% to 50% SRR%, and Stribeck curves with rolling speed from 0 to 2.0 m/s at 50% SRR% were generated at 40 °C, 100 °C, under 30 N and/or 50 N. Following methods provided by PCS Instruments, the MTM ball–disc maximum contact pressure was 0.94 GPa at 30 N load, and 1.11 GPa at 50 N load.

EHD from PCS Instruments is used to measure the film thickness. Steel ball on glass disc, with rolling speed from 0 to 2.0 m/s, 100 °C, under 50 N load. Per the method provided from PCS Instruments, the EHD max ball-disc contact pressure is 0.70 GPa at 50 N.

The DKA oxidation test was performed at 170 °C, with a variable end-of-test (EOT) time up to 192 h, with other parameters as the standard test.

3. Results and Discussion

It is well known that the foaming property of fluids could be regulated by using various types of defoamer additives [22].

Lab tests found that among various types of base oils, most of the low-viscosity (Kinematic viscosity at 100 °C less than 10 cSt) poly alpha olefins (PAOs) from the market, such as SpectraSyn™ Max 3.5, SpectraSyn™ 4, etc., have low air release time (typically less than 20–25 s measured by ASTM D3427 at 50 °C) in comparison to Group III base oils (typically ranging between 100 and 400 s). Some of the low-viscosity PAOs are found to have high air release time similar to that of typical Group IIIs. Blends of low-viscosity PAOs such as PAO2 with PAO6 or PAO7 typically worsen the air release property of the formulations to that of Group III. Certain base oils which are categorized as Group III have low air release time like that of low-viscosity PAOs. This indicates the sensitive nature of the air release properties of the fluid with their chemistry.

Polymer thickeners are used in the formulation to adjust the fluid to the right viscosity. Among polymer thickeners, many are found to have negative effects on air release time with even a small treat rate. For PAO-based EDF formulations, high-viscosity metallocene-based PAOs are found not to affect the air release property at a certain treat rate [23], while having excellent shear stability.

PAOs also have much lower traction coefficient compared to Group II/II+ and IIIs. Thus, right base oil mixes, polymer thickeners, and additive systems were selected to achieve low aeration/traction properties for the EDF formulations covering a wide range of the low-viscosity spectrum to satisfy viscosity requirements, while maintaining the other properties, such as scuffing, wear, shear stability, oxidative stability, electric properties, coating compatibility, and copper corrosion protection. Contrary to intuition that more viscous fluid will have a longer air release time, it is interesting to find that the viscosity of the fluid is not a factor affecting the air release time measured by ASTM D3427, at least for fluids tested ranging between Kv100 = 1.7 cSt and Kv100 = 8.0 cSt (Table 3).

A study of the ATFs and EDFs in the market has shown that their air release time is ranging from 120 to 400 s as measured by ASTM D3427 at 50 °C. ATF fluid reference A has the lowest air release time among them as measured by ASTM D3427 at 50 °C. Reference A and EDF-3 have the same kinematic viscosity, and the same heat transfer capacity shown by the Mo number in a static state. However, under the dynamic driving condition, which is simulated by Fast FZG immersion lubrication, reference A has a much higher aeration (10%) vs. dedicated EDF-3 (<2%) and thus, a poorer heat transfer capacity. It is typical to see other ATFs/EDFs with even higher aeration (10–20%) under different speed steps in the Fast FZG test.

Fast FZG tests (Figure 2) were performed under three speed steps: 6000 rpm for 300 s, 9000 rpm for 180 s, 12,000 rpm for 120 s. Oil conditioning to 40 °C was carried out before starting every step. Other conditions were as follows. Acceleration: 200 rpm/s, constant speed at each speed step, deceleration: 500 rpm/s, 60 s rest. Reference A has higher traction coefficient measured by MTM, higher aeration, and thus poorer heat transfer capacity and higher oil temperature, and a longer Fast FZG test duration, where the total test duration is 3584 s. EDF-3 has a much lower traction coefficient measured by MTM, virtually no aeration under high-speed rpm, and thus excellent heat transfer capacity, close to the Mo number at the static state, lower oil temperature, and shorter Fast FZG test duration, where the total duration is 3030 s. Per Fast FZG protocol, the shortest test duration of the Fast FZG test from start till stop of the last speed step at 12,000 rpm is 2636 s. A shorter test duration means that the fluid tested can transfer the heat better and cool down to 40 °C faster to start the next step. Fluids with higher aeration and poorer heat transfer can have a Fast FZG test duration lasting more than 3800 s. Peak temperature difference for each speed step is between 2 and 8 °C. This will have a significant impact on the performance of the lubricant, such as oxidative stability (oil drain interval, 5 °C lower temperature will be lead to least 80% longer oil drain interval for PAO-based fluids with sump temperature 90 °C as per

the Arrhenius equation with oxidation activation energy of 129.3 kJ/mol [24,25]), electric drivetrain component wear/scuffing (film thickness), and e-motor coating compatibility (temperature-related).

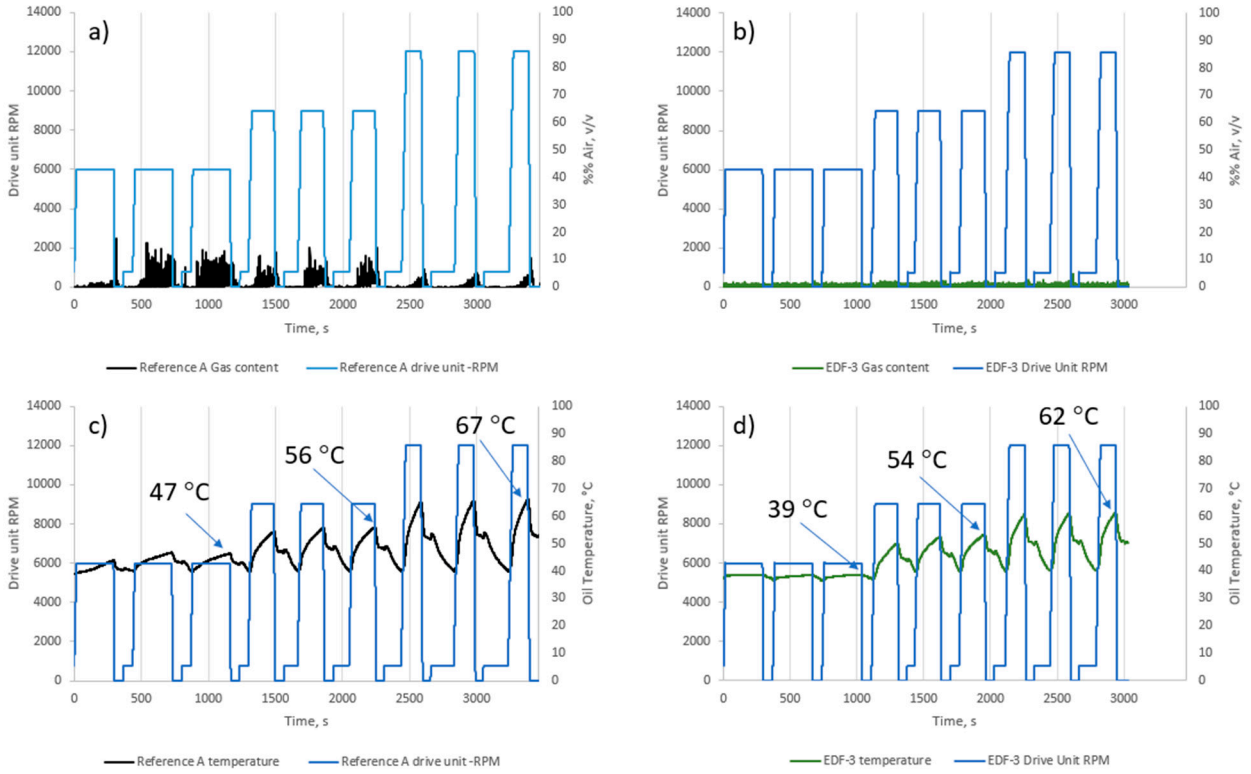

Figure 2. Fast FZG test. Three speed steps under 6000, 9000, 12,000 rpm. Reference A is an off-the-shelf ATF fluid in the market. Fluid peak temperature at the last speed stage is labeled. (**a**) Reference A fluid gas content under three different speed steps. (**b**) EDF-3 gas content under three different speed steps. (**c**) Reference A fluid temperature under three different speed steps. (**d**) EDF-3 gas content under three different speed steps.

Table 3. Low-foaming/aeration low-traction EDF formulations covering wide viscosity range for different OEM design requirements.

Properties	EDF-1	EDF-2	EDF-3	EDF-4	EDF-5	Reference-A
Base oil type	PAO	PAO	PAO	PAO	PAO	Group III
Kv100, cSt, D445	2.53	3.96	4.42	5.95	7.12	4.54
Kv40, cSt, D445	9.12	16.49	18.86	27.41	34.22	19.50
Pour point, °C, D5949	−78	−78	−75	−72	−66	−48
Brookfield viscosity@-40 °C, cP, D2983	1100	1830	2170	3790	5600	-
Foam, ml/mL, D892, Seq. I/II/III	0/0,0/0,0/0	0/0,0/0,0/0	0/0,0/0,0/0	0/0,0/0,0/0	0/0,0/0,0/0	-
Air release@ 50 °C, s, D3427	16	19	17	14	16	120
Air release@ 75 °C, s, D3427	16	14	12	15	18	42
MTM traction, @40% SRR%, @ 50 N, rolling speed from 10 to 1000 mm/s, @100 °C	0.0179	0.0123	0.0123	0.0126	0.0173	0.0236

Table 3. *Cont.*

Properties	EDF-1	EDF-2	EDF-3	EDF-4	EDF-5	Reference-A
DKA, 170 °C, 192 h, EOT KV100% increase	<3%	<3%	<3%	<3%	<3%	14%
DKA, 170 °C, 192 h, EOT Sludge/deposit rating	1	1	1	1	1	1

Under both the Fast FZG high-speed rpm conditions and ASTM D3427 static conditions, air bubbles need to rise to the fluid surface to escape from the system. It is hypothesized that the high-speed aeration is related to the air release time of the fluid by ASTM D3427 in static conditions. Fluids with shorter air release time measured by ASTM D3427 should have a higher chance to yield fluid with lower aeration (<2%) under high-speed rpm in the Fast FZG test. Thus, ASTM D3427 is a fast and easy test to screen before running Fast FZG.

Aeration can significantly reduce the torque efficiency by increasing the friction and power loss between gear teeth, especially at high speeds or under heavy loads. This is also evident in the Fast FZG test (Figure 3).

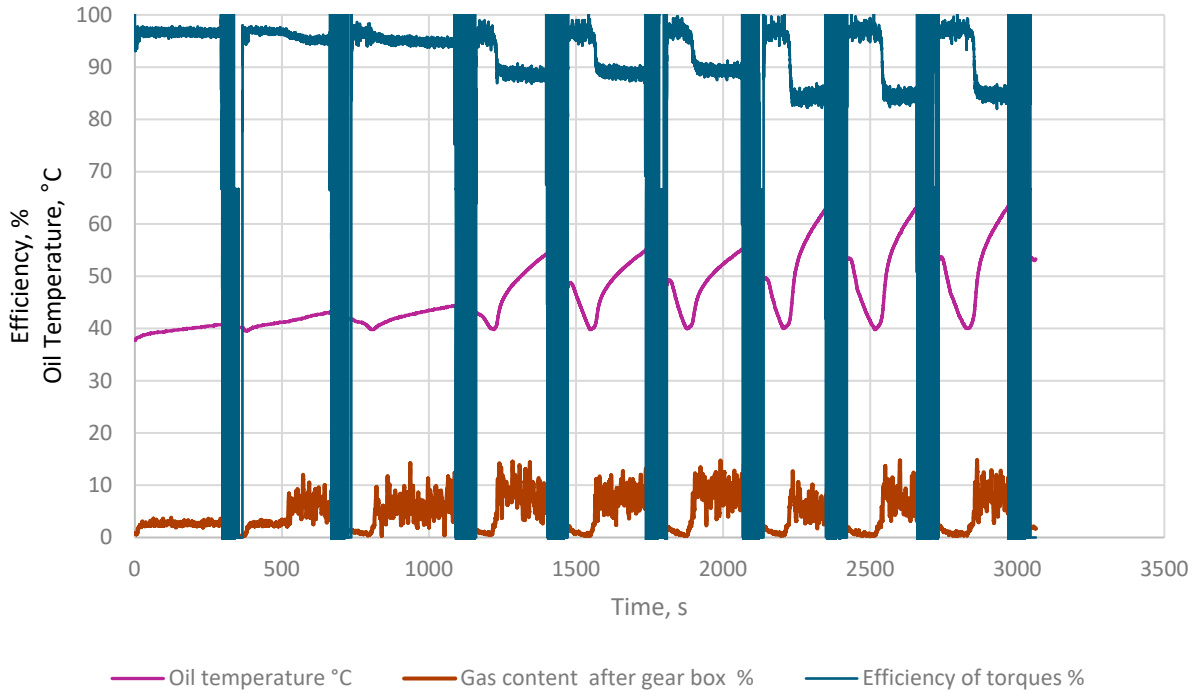

Figure 3. Fast FZG test. Three speed steps under 6000, 9000, 12,000 rpm. Fluid is an experimental PAO-based EDF with Kv100 = 4.9 cSt. Torque efficiency (average of 3 speed steps) decreases with increasing rpm. At 6000 rpm, torque efficiency = 95.8 ± 1.6%. At 9000 rpm, torque efficiency = 89.4 ± 0.5%. At 12,000 rpm, torque efficiency = 85.0 ± 0.5%. When aeration starts to increase in the second 6000 rpm speed step from 2.6 ± 0.4% to 6.5 ± 3.5%, torque efficiency drops from 96.7 ± 0.7% to 94.8 ± 0.5%, and the fluid peak temperature at the end of the 1st 6000 rpm speed step also increases from 40.7 °C to 44.3 °C, clearly showing the negative effect of drop in torque efficiency and increase in power loss due to aeration.

The film thickness of the lubricant is measured by EHD under various temperatures (80 °C, 100 °C, 120 °C, 150 °C) and loads, and PAO-based EDF-3 has slightly higher film thickness at lower rolling speed under various temperatures (Figure 4). The film thickness is typically below 80 nm speed less than 2000 mm/s. The film thickness difference for the fluids with the same viscosity is minimal. Continuous film without a heterogenous phase,

such as any air bubble is critical for bearing and raceway separation. Air has much lower dielectric breakdown voltage, and air bubbles or air holes (broken air bubbles) on the film is a weak point for electric arcing. If there is a lubricant solution to prevent EIBD, then a lubricant with low aeration will be the solution.

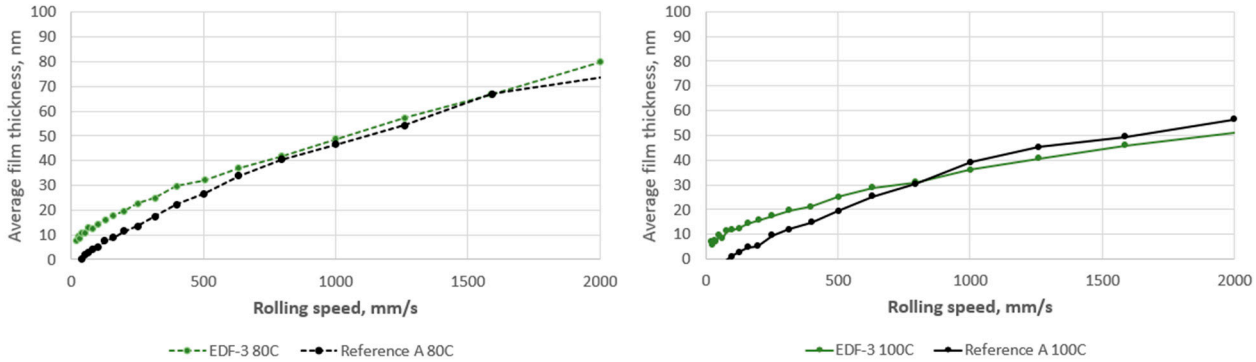

Figure 4. Film thickness measured by EHD at 80 °C and 100 °C at 50 N. Per PCS's provided method, the max contact pressure between the steel ball and the glass disc is 0.70 GPa at 50 N.

Electric motors deliver instant torque and trend towards higher torque, often much higher than internal combustion engines, which places greater stress on gears and bearings. Instant and increased torque also produces higher contact pressure and localized stress between gear teeth, increasing the surface damaging risk such as scuffing. Higher electric motor rotational speeds compared to conventional drivetrains and high-speed aeration may result in thinner film and increase the likelihood of scuffing. Thus, it is desirable for EDFs to have improved load carrying capacity and pitting performance. The EDFs in the study have optimized S/P balance, and the FZG A10/16.6R/90, FZG A10/16.6R/120 FLS are 7, higher compared to traditional ATFs which typically register at FLS around 5. The active sulfur level is reduced; thus, the EDFs have excellent compatibility with copper (ASTM D130 [26], 150 °C, 168 h, EOT copper coupon rating is 4A) and excellent oxidative stability. DKA (170 °C, 192 h) %KV100 increase EOT is less than 3% with excellent sludge and deposit merit rating (Table 3).

It is important for EDFs to maintain low aeration and low traction during usage. This is simulated using aged oil samples. Aged oil samples of reference A and EDF-3 are prepared via DKA oxidation at 170 °C for 48 h and 192 h. EDF-3 maintains fast air release time as measured by ASTM D3427 at 50 °C and 75 °C with no deterioration of air release time (Figure 5).

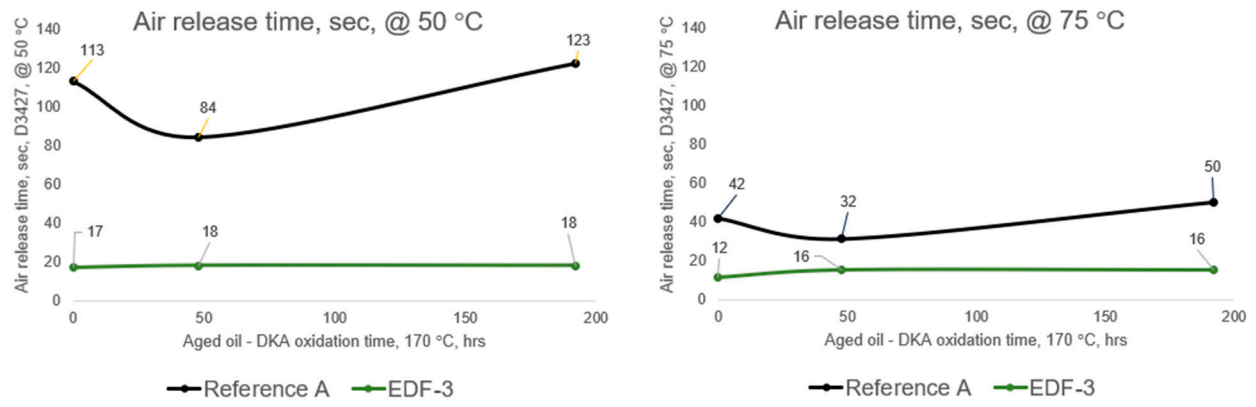

Figure 5. Air release time of aged fluids as measured by ASTM D3427 at 50 °C and 75 °C.

Distilled water also has low dielectric breakdown voltage but higher than that of air [27], and water in the lubricant may contain various levels of impurities that could

further reduce the dielectric breakdown voltage. EDF-3 is spiked with various levels of distilled water to simulate field water contamination and measured by coulometric Karl–Fischer titration, and subsequently, the dielectric breakdown voltage is measured by ASTM D877 Procedure A [28]. It is found that a significant drop of dielectric breakdown voltage occurs when the water level exceeds about 400 ppm (Figure 6). Thus, it is also important for EDFs to have low water content as well. EDF-3 EOT DKA has a water level less than 300 ppm measured by coulometric Karl–Fischer titration.

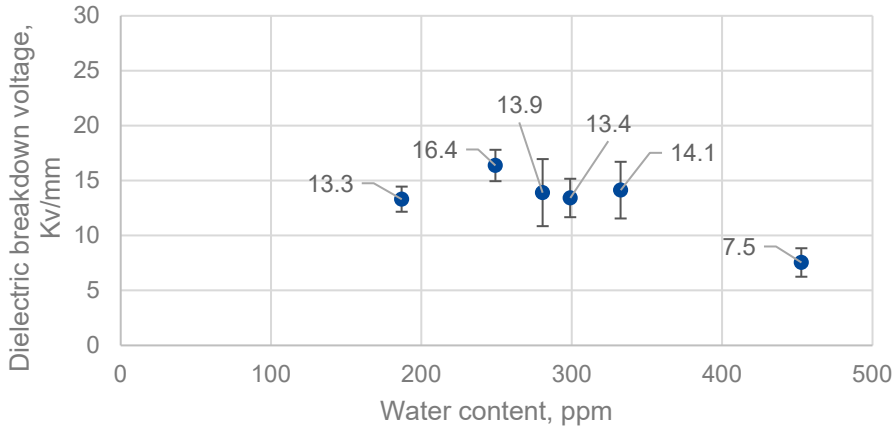

Figure 6. Dielectric breakdown voltage of EDF-3 spiked with various levels of distilled water, measured by ASTM D877 Procedure A, 3 kv/sec ramp rate, 0.10 inch electrode gap, 1 inch disk electrodes, average of 5 runs.

4. Conclusions

Aeration for EDF posed a challenge for a high-speed electric drivetrain. In general, PAO-based fluids have lower traction coefficient and faster air release time in comparison to fluids formulated from Group III type of base oils. By carefully selecting the right components, one could design dedicated EDF formulations to have low traction coefficient and low foaming/aeration. Low traction coefficient and low foaming/aeration fluids under the high-speed condition will have better heat transfer capacity, better energy efficiency, better wear/scuffing protection, better oxidative stability, longer oil drain interval, and longer transmission component life, ideal for direct cooling applications in high-speed electric drivetrains.

Author Contributions: Conceptualization, P.M. and D.M.; methodology, P.M.; validation, C.S.; software, P.M. and C.S.; formal analysis, P.M., D.M., and C.S.; investigation, P.M., D.M., and C.S.; resources, P.M.; writing-original draft preparation, P.M.; writing-review and editing, P.M., D.M. and C.S.; visualization, P.M.; Supervision, P.M.; project administration, P.M.; fund acquisition, P.M. All authors have read and agreed to the published version of the manuscript.

Funding: This research received no external funding.

Data Availability Statement: The original contributions presented in the study are included in the article, further inquiries can be directed to the corresponding author.

Acknowledgments: The authors appreciate the help from Albert Kurz, Rico Pelz, and Gunther Müller from APL on Fast FZG tests.

Conflicts of Interest: The authors declare that this study received funding from BASF Corporation. The funder had the following involvement with the study: study design, collection, analysis, interpretation of data, the writing of this article and the decision to submit it for publication.

References

1. Tuero, A.G.; Rellán, N.R.; Ordóñez, E.R.; Rodríguez, R.G.; Rodríguez, J.L. Can Conventional ATFs Be Used Safely in Electrified Transmissions? In Proceedings of the 77th STLE Annual Meeting, Long Beach, CA, USA, 21–25 May 2023.
2. Ma, P.; Mosher, D.; Steele, C. Low Foaming/Aeration/Traction Synthetic Lubricant Solutions for High-speed Electric Drive-train Fluid. In Proceedings of the 2023 STLE Tribology Frontier & Electric Vehicles Conference, Cleveland, OH, USA, 12–15 November 2023.
3. Mouromtseff, I.E. "Water and Forced-Air Cooling of Vacuum Tubes Nonelectronic Problems in Electronic Tubes. *Proc. IRE* **1942**, *30*, 190–205. [CrossRef]
4. Simons, R.E. Comparing Heat Transfer Rates of Liquid Coolants Using the Mouromtseff Number. *Electron. Cool.* **2006**, *12*, 2.
5. Lenert, A.; Nam, Y.; Wang, E.N. Heat Transfer Fluids. *Annu. Rev. Heat Transf.* **2012**, *15*, 93–129. [CrossRef]
6. Daccord, R.; Kientz, T.; Bouillot, A. Aging of a Dielectric Fluid Used for Direct Contact Immersion Cooling of Batteries. *Front. Mech. Eng.* **2023**, *9*, 1212730. [CrossRef]
7. Rivera, N.; Viesca, J.L.; García, A.; Prado, J.; Lugo, L.; Battez, A.H. Cooling Performance of Fresh and Aged Automatic Transmission Fluids for Hybrid Electric Vehicles. *Appl. Sci.* **2022**, *12*, 8911. [CrossRef]
8. Bergman, T.L.; Lavine, A.S.; Incropera, F.P.; DeWitt, D.P. Table A.6 Thermophysical Properties of Saturated Water. In *Fundamentals of Heat and Mass Transfer*, 7th ed.; John Wiley & Sons, Inc.: Hoboken, NJ, USA, 2011; pp. 1003–1004.
9. Heat Transfer Fluid Data Is from Product Datasheet. Available online: https://www.dow.com/en-us/pdp.dowtherm-g-heat-transfer-fluid.25594z.html#overview (accessed on 15 January 2025).
10. Loos, J.; Bergmann, I.; Goss, M. Influence of High Electrical Currents on WEC Formation in Rolling Bearings. *Tribol. Trans.* **2021**, *64*, 708–720. [CrossRef]
11. Liu, W. The Prevalent Motor Bearing Premature Failures Due to the High Frequency Electric Current Passage. *Eng. Fail. Anal.* **2014**, *45*, 118–127. [CrossRef]
12. Didenko, T.; Pridemore, W.D. Electrical Fluting Failure of a Tri-Lobe Roller Bearing. *J. Fail. Anal. Prev.* **2012**, *12*, 575–580. [CrossRef]
13. Chiou, Y.C.; Lee, R.T.; Lin, S.M. Formation Mechanism of Electrical Damage on Sliding Lubricated Contacts for Steel Pair Under DC Electric Field. *Wear* **2009**, *266*, 110–118. [CrossRef]
14. Ost, W.; Baets, P.D. Failure Analysis of the Deep Groove Ball Bearing of an Electric Motor. *Eng. Fail. Anal.* **2005**, *12*, 772–783. [CrossRef]
15. Prashad, H. Determination of Time Span for the Appearance of Flutes on the Track Surface of Rolling-Element Bearings Under the Influence of Electric Current. *Tribol. Trans.* **1998**, *41*, 103–109. [CrossRef]
16. Hogg, M.G.; Timoshkin, I.V.; MacGregor, S.J.; Wilson, M.P.; Given, M.J.; Wang, T. Electrical Breakdown of Short Non-uniform Air Gaps. In Proceedings of the 19th IEEE Pulsed Power Conference (PPC), San Francisco, CA, USA, 8–12 July 2013; pp. 1–4.
17. LePrince, G.; Changenet, C.; Ville, F.; Velex, P.; Dufau, C.; Jarnias, F. Influence of Aerated Lubricants on Gear Churning Losses-An Engineering Model. *Tribol. Trans.* **2011**, *54*, 929–938. [CrossRef]
18. Hope, K. PAO Contribute to Energy Efficiency in 0W-20 Passenger Car Engine Oils. *Lubricants* **2018**, *6*, 73. [CrossRef]
19. Gunsel, S.; Korcek, S.; Smeeth, M.; Spikes, H.A. The Elastohydrodynamic Friction and Film Forming Properties of Lubricant Base Oils. *Tribol. Trans.* **1999**, *42*, 559–569. [CrossRef]
20. *ASTM D892-18*; Standard Test Method for Foaming Characteristics of Lubricating Oils. ASTM International: West Conshohocken, PA, USA, 2018.
21. *ASTM D3427-19*; Standard Test Method for Air Release Properties of Hydrocarbon Based Oils. ASTM International: West Conshohocken, PA, USA, 2019.
22. Denkov, N.D.; Marinova, K.G.; Tcholakova, S.S. Mechanistic Understanding of the Modes of Action of Foam Control Agents. *Adv. Colloid Interface Sci.* **2014**, *206*, 57–67. [CrossRef] [PubMed]
23. Ma, P.; Mosher, D.; Steele, C. Polyalphaolefin-based Synthetic Gear Lubricants. US Patent Application PCT/US2024/028176, Publication Number WO/2024/233561, 14 November 2024.
24. Shim, J.S.; Cho, W.N.; Chung, K.W. Oxidation Stability of PAO Oils Determined by Differential Scanning Calorimetry. *J. KSTLE* **1996**, *12*, 36–41.
25. Smook, L.A.; Chatra, K.R.S.; Lugt, P.M. Evaluating the Oxidation Properties of Lubricants via Non-isothermal Thermogravimetric Analysis: Estimating Induction Times and Oxidation Stability. *Tribol. Int.* **2022**, *171*, 107569. [CrossRef]
26. *ASTM D130-19*; Standard Test Method for Corrosiveness to Copper from Petroleum Products by Copper Strip Test. ASTM International: West Conshohocken, PA, USA, 2019.

27. Szklarczyk, M.; Kainthla, R.C.; Bockris, J.O. On the Dielectric Breakdown of Water: An Electrochemical Approach. *J. Electrochem. Soc.* **1989**, *136*, 2512–2521. [CrossRef]
28. *ASTM D877*; Standard Test Method for Dielectric Breakdown Voltage of Insulating Liquids Using Disck Electrodes. ASTM International: West Conshohocken, PA, USA, 2019.